Plant Biotechnology 32, 181–191 (2015)
DOI: 10.5511/plantbiotechnology.15.0521a

Original Paper

Peanut stunt virus-induced gene silencing in white lupin (*Lupinus albus*)

Masumi Yamagishi[1,*], Chikara Masuta[1], Masashi Suzuki[2], Osamu Netsu[2,a]

[1] Graduate School of Agriculture, Hokkaido University, N9W9, Kita-ku, Sapporo, Hokkaido 060-8589, Japan;
[2] Graduate School of Frontier Sciences, The University of Tokyo, 5-1-5 Kashiwanoha, Kashiwa, Chiba 277-8562, Japan
* E-mail: yamagisi@res.agr.hokudai.ac.jp Tel: +81-11-706-3846 Fax: +81-11-706-3634

Received April 11, 2015; accepted May 21, 2015 (Edited by K. Kato)

Abstract White lupin (*Lupinus albus* L.) plants develop cluster roots and have strong resistance to phosphorus starvation. Although many expressed sequences have been identified to explain the mechanisms used by white lupin to acquire phosphorus, the lack of a stable transformation technique has made it challenging to evaluate the functions of these expressed sequences. Virus-induced gene silencing (VIGS) is an attractive method for assaying gene function in species that are difficult to stably transform. Here, we show that the *Peanut stunt virus* (PSV) vector effectively induces silencing of endogenous genes in white lupin. It is unknown whether PSV is useful for VIGS; therefore, we first inoculated *Nicotiana benthamiana* plants with PSV harbouring fragments of the *N. benthamiana phytoene desaturase* gene (*NbPDS*). Two out of four distinct sequence fragments of *NbPDS* induced photo-bleaching in *N. benthamiana*, indicating that PSV can be used to knockdown endogenous gene sequences in a sequence-dependent manner. White lupin plants inoculated with PSV harbouring fragments of the *L. albus PDS* gene (*LaPDS*) developed photo-bleaching that was associated with a significant reduction in *LaPDS* mRNA accumulation. PSV spread systemically in leaves, roots, and cluster roots, and small interfering RNA of *LaPDS* was detected in these organs. This is the first study to demonstrate the use of VIGS by PSV, suggesting that this vector can be applied to supress endogenous gene expression in shoots and roots of white lupin and to clarify the mechanisms of phosphorus starvation resistance.

Key words: *Nicotiana benthamiana*, phosphorus acquisition, *phytoene desaturase*, small interfering RNA (siRNA), virus-induced gene silencing (VIGS).

Phosphorus is an essential macronutrient required for plant growth. Although phosphorus is abundant in many types of soil, its availability to plants is limited by slow diffusion and high fixation in soils, because phosphorus often forms insoluble complexes with aluminium and iron. Thus, phosphorus is often a limiting element for plant growth, and fertilisers containing phosphorus derived from mined rock phosphate are essential for high crop productivity. However, mined rock phosphate is a non-renewable resource, and easily accessible mined rock phosphate produced at high quality mines is predicted to be depleted within 50 years. Thus, improvement of phosphorus acquisition and use by plants is critical for its continued application in agricultural practice. Furthermore, a complete understanding of strategies used by plants to acquire phosphorus is important for breeding crop plants with a greater capacity to acquire soil phosphorus (Chiou and Lin 2011; Cordell et al. 2009; Shen et al. 2011; Vance 2010).

White lupin (*Lupinus albus* L.) plants are acclimatised for growth under low-phosphorus conditions and are used as a model plant for the study of phosphorus acquisition. The most recognized adaptation in these plants is the formation of specialized roots that have short, prolific, closely spaced lateral roots (rootlets) of determinate growth (mature rootlets have no meristems), called cluster (or proteoid) roots. Cluster roots increase the uptake of phosphorus from soil by expanding the root surface area and increasing the release of protons, acid phosphatases, carboxylates, and phenolic compounds. Acid phosphatases and carboxylates released from cluster roots solubilize phosphorus compounds in the rhizosphere, thus converting them into an absorbable form (Cesco et al. 2010; Vance et al. 2003; Zhu et al. 2005). Both local and systemic signalling pathways regulate cluster root formation (Cheng et al. 2011b; Neumann 2010; Zhou et al. 2008), and transcription factors and microRNAs have been

Abbreviations: CMV, *Cucumber mosaic virus*; dai, days after inoculation; LMW RNA, low molecular weight RNA; *PDS*, *phytoene desaturase*; PSV, *Peanut stunt virus*; qRT-PCR, quantitative reverse transcription-PCR; RT-PCR, reverse transcription-PCR; siRNA, small interfering RNAs; VIGS, virus-induced gene silencing.

[a] Present address; Graduate School of Agricultural and Life Sciences, The University of Tokyo, 1-1-1 Yayoi, Bunkyo-ku, Tokyo 113-8657, Japan

This article can be found at http://www.jspcmb.jp/
Published online July 16, 2015

isolated and characterised in roots and shoots of white lupin to investigate the signalling networks required to withstand phosphorus deficiency (Tian et al. 2009; Uhde-Stone et al. 2003; Yamagishi et al. 2011; Zhu et al. 2010). Whole-genome transcriptomes have been subjected to next-generation sequencing, and many sequences that are differentially expressed in response to phosphorus deficiency and during cluster root development have been identified (O'Rourke et al. 2013; Secco et al. 2014).

To elucidate the mechanisms used by white lupin to acquire phosphorus, the development of a reverse-genetics tool is required to functionally screen the expressed sequences. Genetic transformation is an essential reverse-genetics tool used to validate the function of endogenous genes. *Agrobacterium*-mediated transformation is widely used to manipulate genes in eudicots and monocots. White lupin plants are recalcitrant to stable transformation: *Agrobacterium tumefaciens*-mediated transformation has not been successful so far. Transformed-hairy roots induced by the infection of *A. rhizogenes* have been used to elucidate the functions of endogenous genes (Cheng et al. 2011a; Sbabou et al. 2010; Uhde-Stone et al. 2005), although shoots cannot be regenerated from hairy roots. Thus, genetic transformation is of limited use for the study of white lupin genes, especially those expressed in shoots. Virus-induced gene silencing (VIGS) is an effective way to transiently knockdown gene expression in plants. Viral double-stranded RNAs, generated during viral replication or by a host RNA-dependent RNA polymerase, trigger post-transcriptional gene silencing and are cleaved by a DICER-like nuclease into small interfering RNAs (siRNAs) consisting of 21–24 nucleotides. siRNAs are then incorporated into RNA-induced silencing complexes (RISCs), and guide them to homologous single-stranded RNAs (ssRNAs) for sequence-specific cleavage of ssRNA targets (Brodersen and Voinnet 2006). If plant cDNA fragments are introduced into the viral genome, corresponding plant mRNAs are cleaved together with the viral genome. This approach is referred to as VIGS, a strategy that can be used to characterise endogenous genes (Senthil-Kumar and Mysore 2011b). The use of VIGS has been well established in studies using model plants and crops, including Leguminosae (Robertson 2004; Senthil-Kumar and Mysore 2011b). In Leguminosae species, *Bean pod mottle virus* (for soybean and common bean), *Pea early browning virus* (for pea and *Medicago truncatula*), *Apple latent spherical virus* (for soybean, pea, and *Vigna* spp.), *Sunnhemp mosaic virus* (for *M. truncatula*), *White clover mosaic virus* (for pea and broad bean), and *Cucumber mosaic virus* (CMV, for soybean) are successfully used to induce VIGS (Constantin et al. 2008; Pflieger et al. 2013), although, to the best of our knowledge, there is no information about the use of VIGS in white lupin.

To use VIGS technology, a viral vector should be selected for the species of interest, because VIGS is only possible in an environment that permits the systemic spread of the viral vector (Pflieger et al. 2013). First, we tested the CMV vector in white lupin because CMV infects a wide range of host plants, including soybean (Nagamatsu et al. 2007), and CMV vectors can induce VIGS in many plant species, including soybean, chilli pepper, tomato, petunia, *Arabidopsis*, and *Nicotiana benthamiana* (Hong et al. 2012; Liu et al. 2010; Matsuo et al. 2007; Nagamatsu et al. 2009; Otagaki et al. 2006). However, we found that CMV-L (leguminous strain, Karasawa et al. 1997) and CMV-Y (ordinary strain, Suzuki et al. 1991) did not spread systemically in white lupin plants (data not shown). Thus, we applied *Peanut stunt virus* (PSV) to white lupin. Taxonomically, PSV is closely related to CMV (a member of the genus *Cucumovirus* in the family *Bromoviridae*) and is infectious for many legume plants, including *Lupinus* species (Obrepalska-Steplowska et al. 2008; Yan et al. 2005). The PSV genome consists of three positive-sense, single-stranded RNA molecules (RNA1, 2, and 3) (Suzuki et al. 2003b). In this study, we modified PSV to develop a VIGS vector and report that this viral vector efficiently induced post-transcriptional gene silencing in white lupin plants.

Materials and methods

Virus and plant materials

PSV-J2, a PSV isolate from Japan, was used as a viral vector. The full-length cDNA molecules of PSV-J2 RNA1, 2, and 3 (GenBank/EMBL/DDBJ accession numbers AB360968, AB360969, and AB360970, respectively) were previously cloned into pUC18 vector (Netsu et al. 2008; Suzuki et al. 2003b). To insert gene fragments into the vector, a cloning site containing *Xba*I, *Nsi*I, *Bgl*II, and *Mlu*I restriction sites was introduced as follows. The full-length cDNA clones of PSV-J2 RNA2 were used as a template. The cloning site was inserted using PCR with mutagenic primers based on the RNA2 sequence from positions 2679–2696 and 2657–2676. Two fragments were amplified using a mutagenic primer based on 2679–2696 and primer positions 2033–2049, and using a mutagenic primer based on 2657–2676 and a 3′ terminal reverse primer. The ends of the two fragments containing the cloning site were annealed and amplified using the primer 2033–2049 containing a *Pst*I recognition site and a 3′ terminal reverse primer containing a *Bam*HI recognition site. The amplified fragments were inserted into full-length cDNA clones of RNA2. The nucleotide positions 2677 and 2678 were replaced by the cloning site sequence (5′-TCT AGA ATG CAT AGA TCT ACG CGT-3′). Therefore, Ser at the last amino acid of the 2b protein was substituted with Phe. The RNA2 construct with the cloning site is shown in Figure 1.

The white lupin 'Kievskij mutant' was hydroponically

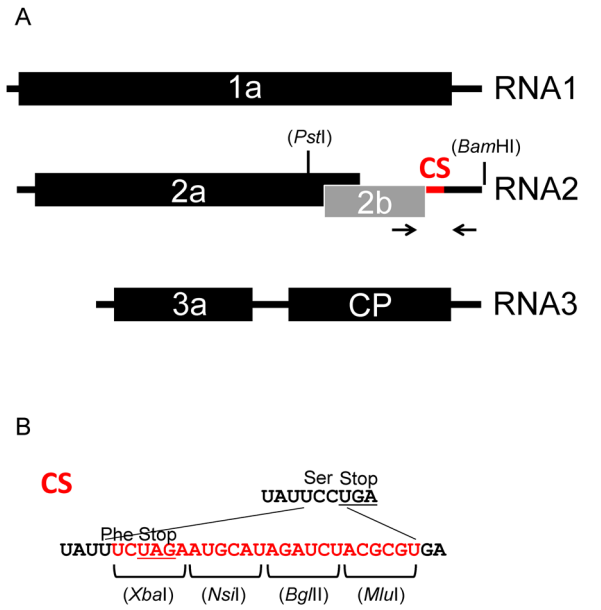

Figure 1. Genome structure of the PSV vector. (A) RNA1, 2, and 3 are the genomic RNAs of PSV. Each of the *PDS* fragments was cloned at a cloning site (CS), which includes recognition sites of *Xba*I, *Nsi*I, *Bgl*II, and *Mlu*I. Arrows indicate the positions of primers used to detect viral inoculation and deletion of the *PDS* fragments. The open reading frame (thicker line) encodes 1a, 2a, 2b, 3a, or CP (coat protein) proteins. (*Pst*I) indicates the recognition site of *Pst*I on the full-length cDNA clones of RNA2. (*Bam*HI) indicates the recognition site of *Bam*HI at the 3′ end of RNA2. The recognition sites of both *Pst*I and *Bam*HI were used for cloning. (B) The nucleotide sequence of CS inserted in RNA2. Since the nucleotides CC at positions 2677 and 2678 were replaced by UC, the last amino acid (Ser) of the 2b protein was replaced by Phe, and a stop codon UGA was replaced by UAG. The underlined region indicates the stop codon of the 2b ORF.

cultivated as previously described (Yamagishi et al. 2011). Seeds of *N. benthamiana* were sown and plants were grown on Jiffy-7® Peat Pellet (Sakata Seed Corporation, Yokohama, Japan). These plants were maintained in a growth incubator at 20°C (white lupin) or 23°C (*N. benthamiana*) under a 16 : 8 h light–dark cycle (fluorescent light).

Isolation of PDS *fragments*

To amplify *phytoene desaturase* (*PDS*) fragments from *N. benthamiana* and white lupin, degenerate primers 5′-GCA AGR GAYGTTYTDGGWGG-3′ (forward) and 5′-RTTRCCA TCY AARAADGCC AT-3′ (reverse) were designed, respectively, from the amino acid sequences ARDVLGG and MAFLDGN conserved in plant *PDS* genes (Yamagishi et al. 2010). In all, 505-bp fragments were amplified by reverse transcription (RT)-PCR, cloned into the pGEM T-Easy vector (Promega, Tokyo, Japan), and then sequenced. A single *N. benthamiana PDS* (*NbPDS*) fragment was obtained, and the sequence was identical to that already registered for *N. benthamiana* (GenBank/EMBL/DDBJ accession number DQ469932). Two *L. albus PDS* sequences, *LaPDS1* and *LaPDS2* (GenBank/EMBL/DDBJ accession numbers AB984615 and AB984616, respectively), were amplified from white lupin leaf cDNA, and were found to share 94% (475/505 bp) identity (Supplementary Figure 1). *LaPDS1* and *LaPDS2* show the highest homology to soybean *PDS* (GenBank/EMBL/DDBJ accession number P28553) with 94% and 95% amino-acid identities, respectively.

Table 1. *PDS* fragments introduced into the PSV RNA2 vector.

Fragment name	Fragment size	Nucleotide position[a]	Orientation
Nicotiana benthamiana PDS			
NbPDS-A	51 bp	34–84	Antisense
NbPDS-B	50 bp	149–198	Antisense
NbPDS-C	50 bp	278–327	Antisense
NbPDS-D	50 bp	373–422	Antisense
NbPDS-2	95 bp	373–467	Antisense
NbPDS-3	145 bp	278–422	Antisense
NbPDS-4	190 bp	278–467	Antisense
NbPDS-5	319 bp	149–467	Antisense
NbPDS-6	434 bp	34–467	Antisense
Lupinus albus PDS			
LaPDS-1	102 bp	320–421	Sense
LaPDS-2	106 bp	278–383	Antisense
LaPDS-3	94 bp	375–468	Antisense

[a] Nucleotide position is illustrated in Figure 2 and Supplementary Figure 1.

Cloning of PDS *fragments into the PSV vector*

Nine *NbPDS* fragments and three *LaPDS* fragments with distinct sequences of different lengths (Table 1) were PCR-amplified using the primers containing either an *Mlu*I or *Xba*I restriction site (Supplementary Table 1). Each *PDS* fragment was cloned into the restriction sites of the PSV-J2 RNA2 vector (Figure 1) via an *Mlu*I/*Xba*I digestion.

Virus inoculation

Before in vitro transcription, the plasmids containing the full-length cDNA of PSV RNA1, 2, and 3 were linearized with *Bam*HI. These plasmids were transcribed with T7 RNA polymerase (Takara, Otsu, Japan), as previously described (Suzuki et al. 2003a, 2003b). Each of the three transcription products and sodium phosphate buffer (pH 7) were mixed in a 1 : 1 : 1 : 7 ratios. Three- to four-week-old *N. benthamiana* leaves were dusted with carborundum (400 mesh, Nacalai Tesque, Osaka, Japan) and inoculated with the virus by rubbing with the mixture containing the vector (25 μl per plant). White lupin plants were inoculated with PSV twice at approximately 3 and 10 days after emergence: *N. benthamiana* leaves harbouring PSV were harvested and ground with the phosphate buffer to produce leaf sap, and true leaves of white lupin were dusted with carborundum and inoculated by rubbing with the leaf sap. In the first and second inoculations, different true leaves were used.

RT-PCR

For RT-PCR, total RNA was isolated from *N. benthamiana* and white lupin leaves by using an RNeasy Plant Mini Kit (Qiagen, Tokyo, Japan), according to the manufacturer's instructions. cDNA was synthesized with SuperScript III reverse transcriptase (Invitrogen, Tokyo, Japan) or M-MLV reverse transcriptase (Takara) by using approximately 2 μg of total RNA

and the following primers 5′-CAT TGT ACA CGG CTC TTC AC-3′ (for viral detection) or oligo $(dT)_{17}$ (for *PDS* amplification). First strand cDNA was diluted 10× and used as a PCR template.

Successful infection of the *N. benthamiana* and white lupin plants with PSV was confirmed by amplification of viral RNA by RT-PCR. The primer sequences 5′-CCT CCT CCA CGA CGA AGA TA-3′ (forward) and 5′-CAT TGT ACA CGG CTC TTC AC-3′ (reverse) anneal to the flanking sequences of the cloning site of the RNA2 vector (Figure 1) and were used to confirm deletion of the inserted *PDS* sequences.

LaPDS transcript levels in white lupin plants were evaluated by quantitative RT (qRT)-PCR. Each PCR reaction was performed in a final volume of 20 μl containing 10 μl of 2× SYBR Premix Ex Taq (Takara), 2 μl of template cDNA, and 0.2 μM of each primer. Signal intensity was monitored by the Chromo4 real-time PCR system (Bio-Rad, Tokyo, Japan). Primer specificity was confirmed by melting curve analysis and agarose gel electrophoresis of the qRT-PCR products. The amount of *LaUbiquitin* (GenBank/EMBL/DDBJ accession number CA410752) mRNA (Uhde-Stone et al. 2003) in each sample was determined and used as an internal control. Relative fold differences of the target sequence were calculated based on the $2^{-\Delta Ct}$ method, where $\Delta Ct = Ct$ (*LaPDS*) $- Ct$ (*LaUbiquitin*) (Livak and Schmittgen 2001). Primer sequences were as follows: 5′-GGT TGC TGC ATG GCA AGA TG-3′ (forward) and 5′-CCA AGT TCT CCA AAC AGG TTC-3′ (reverse) for *LaPDS* and 5′-TCT TTG TGA AGA CCC TCA CC-3′ (forward) and 5′-CTG CTG GTC CGG AGG AAT G-3′ (reverse) for *LaUbiquitin*.

Detection of siRNA by stem-loop pulsed RT and end-point PCR

Low molecular weight (LMW) RNA was isolated from leaves, roots, and cluster roots of white lupin plants using a High Pure miRNA Isolation kit (Roche Diagnostics K.K., Tokyo, Japan) according to the manufacturer's instructions. siRNAs were transcribed into cDNA using the stem-loop pulsed RT protocol (Varkonyi-Gasic et al., 2007). The mixture containing approximately 40 ng LMW RNA, 0.05 μM stem-loop RT primer, and 0.25 mM dNTP was heated to 65°C for 5 min and cooled on ice for 2 min. After adding 0.5 μl of RNase inhibitor, 1 μl of PrimeScriptII reverse transcriptase (Takara), and 4 μl of 5× buffer (20 μl in total volume), pulsed RT was performed: incubation at 16°C for 30 min, 60 cycles of 30°C for 30 s, 42°C for 30 s, and 50°C for 1 s, followed by heat-inactivation of the reverse transcriptase at 85°C for 10 min. Then, end-point PCR (Varkonyi-Gasic et al., 2007) was carried out in a reaction solution containing 1 μl of the cDNA solution, 0.2 μM foreword primer, 0.2 μM universal reverse primer (5′-GTG CAG GGT CCG AGG T-3′), 1× buffer, 0.2 mM dNTP, and Ex Taq DNA polymerase (Takara), which was incubated at 94°C for 2 min, and subjected to 35 cycles of 94°C for 15 s, and 60°C for 1 m. PCR products were separated on 4% agarose gel. siRNA sequences of *LaPDS* (siR1–siR5) were presumed according to the algorithm postulated by Ui-Tei et al. (2004) and Reynolds et al. (2004); for example, A or U at the 5′ terminal of the guide strand, G or C at the 5′ terminal of the passenger strand, and base preferences at positions 3 (A), 10 (U), and 13 (A, U, or C) of the passenger strand. A combination of stem-loop RT primers and reverse PCR primers are shown in Table 2.

To confirm the presence of the LMW RNA, U6 small nuclear RNA was amplified: The LMW RNA was reverse transcribed using a reverse primer (5′-CGA TTT GTG CGT GTC ATC CTT GC-3′) and then amplified by PCR using a forward primer (5′-CGG GGA CAT CCG ATA AAA TTG GAA CG-3′) and the same reverse primer.

Results

VIGS of phytoene desaturase gene in N. benthamiana

It is unknown whether PSV can induce VIGS therefore, we first characterised PSV as a VIGS vector using *N.*

Table 2. Sequences of siRNAs (siR1–siR5) and primers used for stem-loop pulsed RT and end-point PCR (5′–3′).

A part of antisense sequence of the LaPDS-3 fragment		
…TGAAGTTGAGTGCCTTTGACATTGCTATGAACACCTCATCAGTTACTCGTTCAG…		
siR1	siRNA sequence	*TGAGTGCCTTTGACA*TTGCTA
	Stem-loop RT primer	GTTGGCTCTGGTGCAGGGTCCGAGGTATTCGCACCAGAGCCAACTAGCAA
	Forward PCR primer	TCGCG*TGAGTGCCTTTGACA*
siR2	siRNA sequence	*TTGACATTGCTATGA*ACACCT
	Stem-loop RT primer	GTTGGCTCTGGTGCAGGGTCCGAGGTATTCGCACCAGAGCCAACAGGTGT
	Forward PCR primer	TCGCG*TTGACATTGCTATGA*
siR3	siRNA sequence	*TGACATTGCTATGAA*CACCTC
	Stem-loop RT primer	GTTGGCTCTGGTGCAGGGTCCGAGGTATTCGCACCAGAGCCAACGAGGTG
	Forward PCR primer	TCGCG*TGACATTGCTATGAA*
siR4	siRNA sequence	*TTGCTATGAACACCT*CATCAG
	Stem-loop RT primer	GTTGGCTCTGGTGCAGGGTCCGAGGTATTCGCACCAGAGCCAACCTGATG
	Forward PCR primer	TCGCG*TTGCTATGAACACCT*
siR5	siRNA sequence	*TGAACACCTCATCAG*TTACTC
	Stem-loop RT primer	GTTGGCTCTGGTGCAGGGTCCGAGGTATTCGCACCAGAGCCAACGAGTAA
	Forward PCR primer	TCGCG*TGAACACCTCATCAG*

Reverse complimentary sequences are underlined, and same forward sequences are in italic.
A universal reverse PCR primer in all cases is: GTGCAGGGTCCGAGGT.

benthamiana. *N. benthamiana* plants were inoculated with PSV harbouring fragments of the *N. benthamiana* phytoene desaturase gene (*NbPDS*). *PDS* encodes an enzyme essential for carotenoid biosynthesis and provides a visual reporter for silencing because its suppression results in chlorophyll photo-bleaching in the affected tissues (Kumagai et al. 1995).

Four fragments of length 50 or 51 bp, with distinct sequences designated as NbPDS-A, NbPDS-B, NbPDS-C, and NbPDS-D (Table 1, Figure 2A), were inserted into the PSV RNA2 vector. Viral infection of *N. benthamiana* plants was confirmed by RT-PCR by using total RNA from the developing leaves sampled above the site of inoculation (systemic leaves) and PCR primers that amplified the RNA2 sequence spanning the cloning site (Figure 1). In all PSV-inoculated plants, single viral RNA fragments of the predicted sizes were amplified (Figure 2B). *N. benthamiana* plants inoculated with PSV harbouring NbPDS-C and NbPDS-D exhibited a photo-bleaching phenotype approximately 17 days after inoculation (dai), while those with PSV harbouring NbPDS-A and NbPDS-B remained green (Figure 2C). All leaves of plants inoculated with PSV lacking the *NbPDS* insert sequences (empty vector; hereafter, Empty) and those of mock-inoculated plants (rubbed with buffer only; hereafter, Mock) remained green (Figure 2D). Weak viral symptoms such as a slightly lumpy leaf surface were observed on systemic leaves in Empty plants and those that harboured *NbPDS* fragments (Figure 2D). These results indicate that the PSV vector can induce gene silencing in *N. benthamiana* without inducing severe symptoms of viral infection and that the induction of gene silencing depends on the position of fragments or sequences of endogenous genes.

To confirm the insert length required for effective silencing, *NbPDS* fragments of several lengths, 50 bp (NbPDS-D), 95 bp (NbPDS-2), 145 bp (NbPDS-3), 190 bp (NbPDS-4), 319 bp (NbPDS-5), and 434 bp (NbPDS-6) were inserted into the PSV RNA2 vector (Table 1). All of these fragments included an NbPDS-D sequence. Nearly all of the *N. benthamiana* plants inoculated with PSV harbouring these fragments exhibited photo-bleaching of systemic leaves (Figure 3A). Because inserted gene fragments are often deleted during systemic viral infection (Yuan et al. 2011), the stability of *PDS* fragments inserted in RNA2 in *N. benthamiana* plants was confirmed by RT-PCR by using total RNA

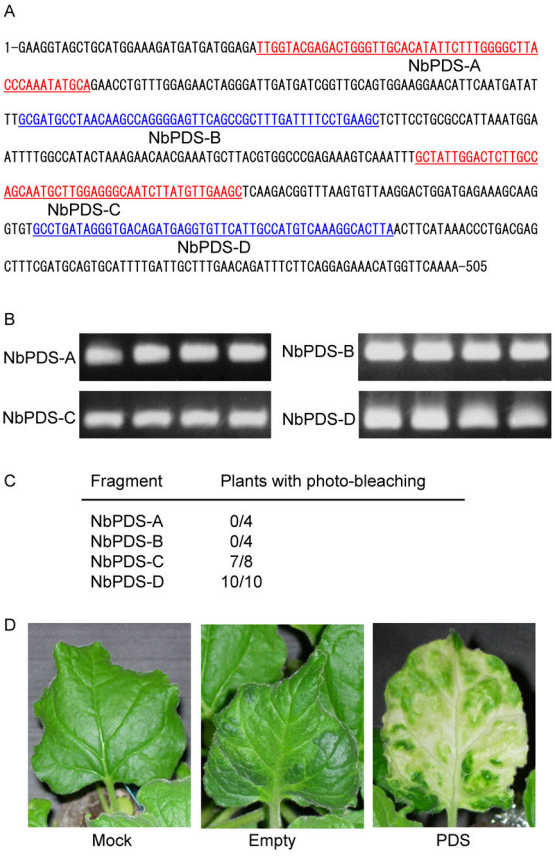

Figure 2. VIGS of *NbPDS* in *N. benthamiana* plants is affected by the position of the target gene. (A) Nucleotide sequence of *NbPDS* (partial). Regions introduced into PSV RNA2 are underlined. (B) RT-PCR analysis amplified the PSV RNA2 region, including a cloning site to confirm the viral infection. Results from four plants are shown for each vector construct. (C) Frequency of plants showing the photo-bleaching phenotype. (D) Representative upper (systemic) leaves of plants inoculated with PSV empty vector (Empty plants) or with PSV carrying an *NbPDS* fragment (PDS). A Mock plant was rubbed with buffer only (17 dai).

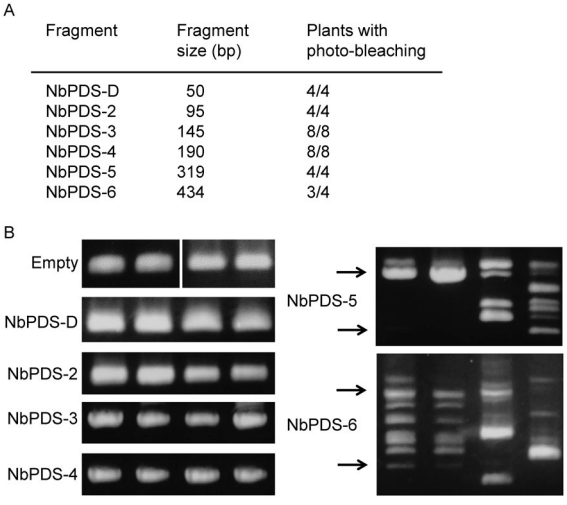

Figure 3. Effect of the fragment size of *NbPDS* on silencing efficiency and the stability of foreign gene fragments in *N. benthamiana* plants. (A) Fragment size and the frequency of plants with photo-bleaching (17 dai). (B) RT-PCR analysis amplified the PSV RNA2 region including a cloning site to confirm insertion of the *PDS* fragment. Single fragments of the expected size were amplified in Empty, NbPDS-D, NbPDS-2, NbPDS-3, and NbPDS-4, whereas many fragments appeared in NbPDS-5 and NbPDS-6. The upper arrow indicates the expected size including full NbPDS-5 or NbPDS-6 fragments, and the lower arrow indicates vector size with no foreign gene fragments. RNA was isolated from upper systemic leaves and four plants were analysed for each construct.

from the upper systemic leaves and the PCR primers described above. Single fragments with the expected size were amplified from Empty plants or those harbouring NbPDS-D, NbPDS-2, NbPDS-3, and NbPDS-4, indicating that *PDS* fragments in the RNA2 vector were stable (not deleted) during systemic viral infection in *N. benthamiana* plants. However, of the four plants with PSV harbouring NbPDS-5, a single fragment with the expected size was amplified in two plants, and several different-sized fragments were detected in the other two plants. In the plants inoculated with PSV harbouring NbPDS-6, several fragments were amplified in all four plants (Figure 3B). Fragments of unexpected sizes may be caused by the deletion of inserted *PDS* fragments and/or rearrangement around the cloning site. These results indicate that size constraints of insert (target gene) fragments exist in the PSV VIGS vector and that insert fragments shorter than 190 bp are stable in host plants, whereas those longer than 319 bp are not.

VIGS in white lupin

Two partial cDNA sequences of *PDS*, *LaPDS1* and *LaPDS2*, were amplified from *L. albus* leaves using degenerate primers (Supplementary Figure 1). Because white lupin is an autogamous crop and its cultivars are genetically homozygous, this suggests that *LaPDS1* and *LaPDS2* are different genes (not allelic). These sequences shared 94% (475/505 bp) homology. Holzberg et al. (2002) observed photo-bleaching in barley plants infected with the *barley stripe mosaic virus* expressing barley, rice, or maize *PDS* fragments and reported that sequences sharing 88–100% identity with the endogenous gene target cause silencing. Thus, the *LaPDS1* sequence was used in this study to knockdown both *PDS* genes in white lupin.

Three *LaPDS* fragments, including sequences homologous to those of NbPDS-C or NbPDS-D of *N. benthamiana*, were cloned into the PSV RNA2 vector in sense (LaPDS-1) or antisense (LaPDS-2 and LaPDS-3) orientations (Table 1). At 90–100 dai, photo-bleaching could be observed around the veins of upper systemic leaves (Figure 4B). Photo-bleaching was observed in 32–38% of white lupin plants (Figure 4A), whereas Empty plants did not exhibit photo-bleaching. Single PSV RNA2 fragments were amplified by RT-PCR in the systemic leaves of white lupin plants inoculated with PSV: a smaller fragment than expected appeared in one plant inoculated with PSV with LaPDS-1, and fragments with the expected size were detected in other plants (Figure 4C). No clear difference appeared in the orientations (sense or antisense) of endogenous genes (Figure 4A). Almost no symptoms of PSV infection were observed in infected white lupin plants. Plants exhibiting a photo-bleached phenotype, as well as Empty plants developed seeds (data not shown). Accumulation of *LaPDS* mRNA

A

Fragment	Fragment size (bp)	Sense or anti-sense	Plants showing photo-bleaching
LaPDS-1	102	Sense	3/8 (38%)
LaPDS-2	106	Anti-sense	7/20 (35%)
LaPDS-3	94	Anti-sense	6/19 (32%)

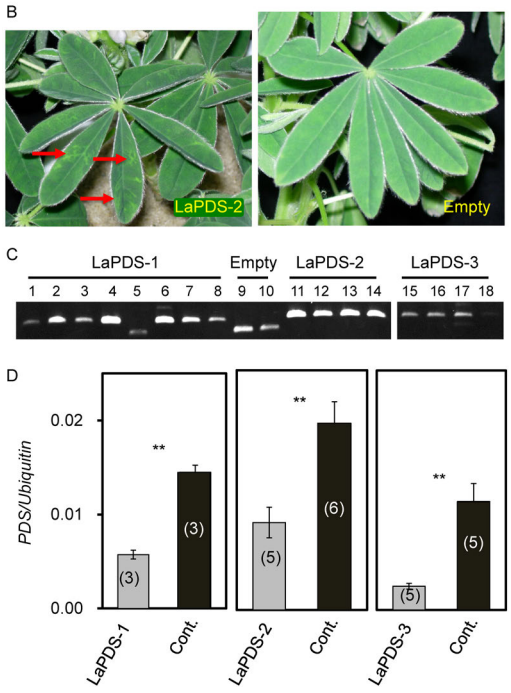

Figure 4. VIGS of *LaPDS* in white lupin (*L. albus*) plants. (A) Frequency of plants showing the photo-bleaching phenotype. (B) Representative upper systemic leaves of plants inoculated with PSV carrying a LaPDS-2 fragment (LaPDS-2) or with PSV empty vector (Empty) at 90 dai. Arrows indicate the regions exhibiting photo-bleaching. (C) RT-PCR analysis amplified the PSV RNA2 region, including a cloning site to confirm insertion of the *PDS* fragment (71 dai). Results from eight (LaPDS-1), four (LaPDS-2), four (LaPDS-3), and two (Empty) plants are shown. In one of the eight LaPDS-1 plants (plant #5), a single fragment with a smaller size was amplified. A single fragment was detected in plant #18 (LaPDS-3), although its expression was very low. (D) Relative transcription of *LaPDS* in VIGS photo-bleached leaves of white lupin plants inoculated with PSV harbouring LaPDS-1, LaPDS-2, or LaPDS-3 fragments. Control plants (Cont.) include those inoculated with PSV without *LaPDS* (Empty) and those rubbed with buffer only (Mock). The levels of *LaPDS* transcription were analysed by qRT-PCR, and *LaUbiquitin* was used to normalize the expression of the gene under identical conditions. Numbers of plants evaluated are shown in parenthesis. Vertical bars indicate the standard error. ** indicates significant difference at the 1% level (*t*-test).

was quantified by qRT-PCR by using RNA isolated from upper systemic leaves. In this experiment, control plants consisted of Empty and Mock plants because these plants showed the similar transcription levels. Relative expression of *LaPDS* in white lupin plants exhibiting photo-bleaching was 19–49% of that in the control plants (Figure 4D), suggesting that reduced levels of *LaPDS* transcription may be responsible for the photo-bleached phenotype.

To further characterise VIGS in white lupin plants, plants were additionally inoculated with PSV harbouring

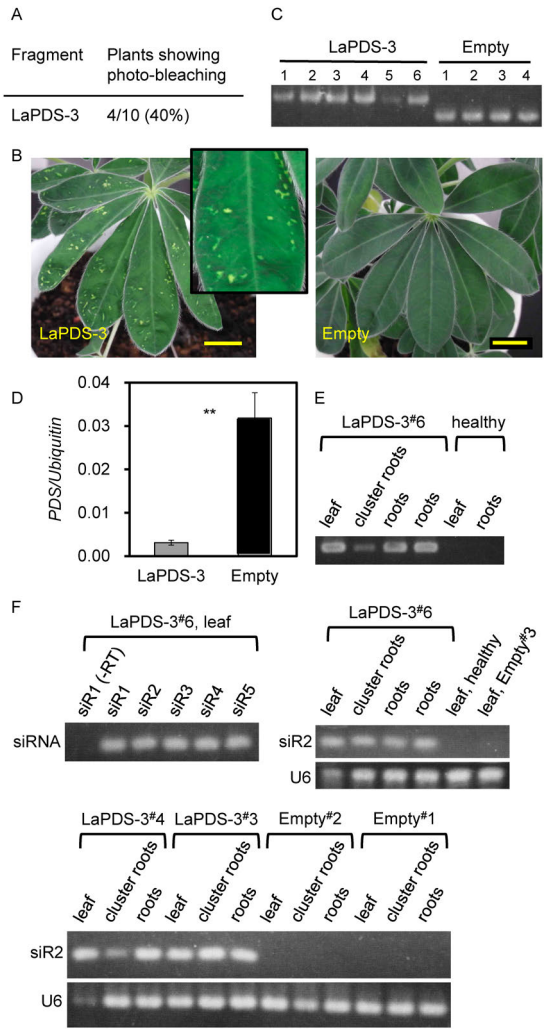

Figure 5. Detection of virus infection and siRNA in shoots and roots of white lupin (*L. albus*) plants inoculated with PSV harbouring a LaPDS-3 fragment. (A) Frequency of plants exhibiting the photo-bleaching phenotype (28 dai). (B) Representative upper systemic leaves of plants inoculated with PSV carrying a LaPDS-3 fragment (LaPDS-3) or with PSV empty vector (Empty) at 28 dai. (C) RT-PCR analysis amplified the PSV RNA2 region including a cloning site to confirm insertion of the *PDS* fragment at 15 dai. Results from six (LaPDS-3) and four (Empty) plants are shown. (D) Relative transcription of *LaPDS* in VIGS photo-bleached leaves of four LaPDS-3 plants and in green leaves of three Empty plants. *LaPDS* transcript levels were analysed by qRT-PCR, and *LaUbiquitin* was used to normalize the expression of the gene under identical conditions. Vertical bars indicate the standard error of the means of four or three plants. ** indicates significant difference at the 1% level (*t*-test). (E) Detection of PSV infection (RNA2 region) in leaves, cluster roots, and roots (two different parts) of the LaPDS-3 plant (plant #6 in panel C) and in the leaves and roots of a healthy plant. (F) Detection of five siRNA molecules (siR1–siR5, Table 2) in a leaf of the LaPDS-3 plant #6 and siR2 in leaves, cluster roots, roots of the LaPDS-3 plants and of healthy and Empty plants. Fragments of U6 small nuclear RNA were amplified from LMW RNA used for siRNA detection.

the LaPDS-3 fragment (Figure 5). Photo bleaching began to appear at 15 dai, and 4 of 10 plants exhibited the photo-bleaching phenotype at 28 dai. Virus fragments with or without the LaPDS-3 fragment were detected in all of the LaPDS-3 and Empty plants, respectively (Figure 5C). *LaPDS* transcript levels in LaPDS-3 plants exhibiting the photo-bleaching phenotype were approximately 10% of that in the Empty plants (Figure 5D). Virus infection and the generation of siRNA were analysed in leaves and roots. Viral fragments were detected by RT-PCR in the leaves, roots, and cluster roots of a PSV-inoculated plant, whereas no fragments were detected in the leaves and roots of a healthy plant, indicating that the virus spread systemically in roots as well as in cluster roots (Figure 5E). siRNA molecules of *LaPDS1* were detected by stem-loop pulsed RT and end-point PCR methods. All of the five presumed siRNA molecules (siR1–siR5, Table 2) were PCR-amplified from the LaPDS-3 leaves (Figure 5F). These amplified fragments of siR1–siR5 were confirmed by sequencing, and the 21-nucleotide siRNA sequences were included in the 60-bp amplified fragments (data not shown). In addition, these siRNA molecules were detected in the leaves, cluster roots, and roots of three LaPDS-3 plants, but amplified fragments did not appear in the same organs of healthy and Empty plants (siR2 products are representatively shown in Figure 5F), indicating that *LaPDS* siRNA accumulates in shoots, cluster roots, and roots of VIGS-induced plants. Taken together, these results indicate that PSV spread systemically from the initial sites of infection to the upper developing leaves, roots, and cluster roots, and that PSV can be used as a vector to induce post-transcriptional gene silencing in shoots and roots of white lupin.

Discussion

A number of expressed sequences have been identified in white lupin to clarify the mechanisms involved in cluster root development and strong phosphorus acquisition (O'Rourke et al. 2013; Secco et al. 2014; Uhde-Stone et al. 2003). To accelerate the functional characterisation of white lupin genes, the development of a reverse-genetics tool is required. VIGS is an attractive reverse-genetics tool for use in plants that are recalcitrant to stable transformation. In this study, we show that PSV successfully induced silencing of *LaPDS* genes in white lupin.

Systemic viral infection is essential to achieve VIGS. Although CMV has been applied to induce gene silencing in a wide range of plant species, including legume species, CMV was unable to spread systemically in white lupin plants in our preliminary experiment (data not shown). Thus, we used PSV as a viral vector in this study because PSV is infectious to many legume plants, including *Lupinus* species, and show that PSV can spread in white lupin plants. Because PSV and CMV are closely related virus species (Suzuki et al. 2003b), we treated PSV in exactly the same way as we would CMV. Therefore,

host plant gene fragments were introduced just downstream of a stop codon of the 2b ORF (Figure 1), consistent with the method used to develop CMV vectors to prevent the deleterious effects of extra fragments on systemic viral infection (Hong et al. 2012; Kanazawa et al. 2011; Otagaki et al. 2006). Plants can be inoculated with PSV and CMV by rubbing the leaves with virus solution. *Agrobacterium*-infiltration and biolistic delivery of viral vectors (Pflieger et al. 2013) are not necessary for PSV inoculation and other special methods such as vacuum-infiltration (Di Stilio et al. 2010; Yan et al. 2012; Zhong et al. 2014) are dispensable to this VIGS system. Thus, the ease of inoculation would be advantageous for the large scale screening of endogenous gene functions.

The white lupin genes predicted to be involved in cluster root development and in phosphorus acquisition are transcribed in roots, shoots, or whole plant bodies (O'Rourke et al. 2013; Secco et al. 2014; Zhu et al. 2010). Thus, gene-silencing systems that can knockdown genes in both roots and shoots are desirable as they permit the functional study of such genes. In the PSV VIGS system, PSV spread systemically in leaves, roots, and cluster roots, and *LaPDS* siRNA accumulated in these organs (Figure 5), indicating that the VIGS system can supress target gene expression in the whole plant and that it should have higher utility than other gene silencing systems previously developed in white lupin. In some VIGS vectors, the virus cannot invade roots, and some modifications are required to induce silencing in this organ. For example, inclusion of the 2b gene greatly improves the capacity of the tobacco rattle virus vector to invade root systems (Valentine et al. 2004), and a novel agroinoculation method, agrodrench, improves the efficiency of VIGS in roots (Ryu et al. 2004). Our PSV vector displayed pervasive systemic invasion in roots without the requirement of any modifications, which is advantageous for VIGS-based functional characterization of genes expressed in roots.

In white lupin plants, photo-bleaching could be observed around the veins of upper systemic leaves (Figures 4 and 5). Similar photo-bleaching phenotypes caused by *PDS* gene silencing have been reported in *N. benthamiana* and *Brachypodium distachyon* plants inoculated with *Bamboo mosaic virus* and its satellite RNA vectors (Liou et al. 2014) and in citrus plants infected with *Citrus leaf blotch virus* vector (Agüero et al. 2014). One possible explanation for the vein-restricted photo-bleaching phenotype in white lupin plants is that PSV was hard to spread to whole leaflets and existed in or around veins. Himber et al. (2003) experimentally showed that silencing of endogenous genes induced by *Potato virus X* (PVX) is restricted to 10–15 cells around the veins if PVX genome lacks 25 kDa protein, which is required for the cell-to-cell spread of the virus, resulting in phloem restriction of the virus. In this study, photo-bleaching appeared on whole lamina in *N. benthamiana* plants, but was restricted to the vicinity of veins in white lupin plants, suggesting that the restricted spread should be caused by the interaction of PSV with white lupin plants: further experiments will be necessary to examine this possibility.

In VIGS systems, silencing phenotypes often appear 3–4 weeks after infection, but can sometimes appear at >6 weeks after inoculation (Di Stilio et al. 2010; Tian et al. 2014; Zhong et al. 2014). In this study, *N. benthamiana* plants exhibited the photo-bleaching phenotype at approximately 17 dai (Figure 2). In white lupin plants, photo-bleaching appeared at 90–100 dai in the experiment shown in Figure 4 and at 15–28 dai in the experiment shown in Figure 5, indicating that the duration required for the expression of photo-bleaching was very different. The intensity of fluorescent light in the growth incubator was weaker in the former experiment, which could explain the longer duration. Growth conditions such as light and temperature promote good viral spread and effective silencing (Burch-Smith et al. 2004, 2006; Senthil-Kumar and Mysore 2011a; Tuttle et al. 2008).

In VIGS systems, it is important that the VIGS vector induces no or few symptoms of viral infection because virus symptoms sometimes disturb the loss-of-function phenotype associated with the silenced target gene (Pflieger et al. 2013; Senthil-Kumar and Mysore 2011b). In this investigation, very few symptoms of PSV infection were observed in white lupin plants infected with a PSV vector harbouring *LaPDS* fragments or in Empty plants. Thus, the PSV VIGS system is suitable for the study of functional genomics in white lupin.

The PSV vector was characterized using *N. benthamiana*. To determine the optimal length of gene fragments required for silencing, various lengths of *NbPDS* fragments were investigated (Figure 3). The results indicate that there are size constraints of insert fragments in the PSV VIGS vector and that 50–190 bp is the optimal length needed to induce silencing. The size constraints of insert fragments have also been reported in other viral vector systems, where vectors with larger inserts are more susceptible to losing the inserts within the plants (Hsieh et al. 2013; Huang et al. 2009; Igarashi et al. 2009; Liu and Page 2008; Peele et al. 2001; Senthil-Kumar and Mysore 2011b; Yuan et al. 2011).

Silencing efficiency was affected by the position or sequence of *PDS* (Figure 2), indicating that the position of the target gene region is important for efficient VIGS induction. These results are consistent with those obtained using other viral systems (Constantin et al. 2008; Liu and Page 2008; Zhang et al. 2010). In addition to the insert size and position of target genes, the effect of the cloning orientation of the foreign gene was investigated using white lupin plants. No clear differences

were detected between sense and antisense orientations in this study (Figure 4), although antisense fragments have been shown to be more effective for silencing in other VIGS systems (Igarashi et al. 2009; Pflieger et al. 2008; Zhang et al. 2010).

In conclusion, to our knowledge, this is the first report of the development of PSV as a VIGS vector. Our results confirm that the PSV VIGS system can be used to introduce gene fragments up to 190 bp in size and can efficiently suppress the transcription of endogenous genes in white lupin. The spread of PSV and siRNA in leaves, roots, and cluster roots enables this system to suppress gene expression in whole plant bodies. The use of the PSV VIGS technique in white lupin plants will facilitate the functional screening of genes necessary for phosphorus acquisition in this species.

Acknowledgements

This work was supported by a Grant-In-Aid for Scientific Research (no. 17658032) from the Japan Society for the Promotion of Science.

References

Agüero J, Vives MC, Velázquez K, Pina JA, Navarro L, Moreno P, Guerri J (2014) Effectiveness of gene silencing induced by viral vectors based on *Citrus leaf blotch virus* is different in *Nicotiana benthamiana* and citrus plants. *Virology* 460–461: 154–164

Brodersen P, Voinnet O (2006) The diversity of RNA silencing pathways in plants. *Trends Genet* 22: 268–280

Burch-Smith TM, Anderson JC, Martin GB, Dinesh-Kumar SP (2004) Applications and advantages of virus-induced gene silencing for gene function studies in plants. *Plant J* 39: 734–746

Burch-Smith TM, Schiff M, Liu Y, Dinesh-Kumar SP (2006) Efficient virus-induced gene silencing in Arabidopsis. *Plant Physiol* 142: 21–27

Cesco S, Neumann G, Tomasi N, Pinton R, Weisskopf L (2010) Release of plant-borne flavonoids into the rhizosphere and their role in plant nutrition. *Plant Soil* 329: 1–25

Cheng L, Bucciarelli B, Liu J, Zinn K, Miller S, Patton-Vogt J, Allan D, Shen J, Vance CP (2011a) White lupin cluster root acclimation to phosphorus deficiency and root hair development involve unique glycerophosphodiester phosphodiesterases. *Plant Physiol* 156: 1131–1148

Cheng L, Bucciarelli B, Shen J, Allan D, Vance CP (2011b) Update on lupin cluster roots. Update on white lupin cluster root acclimation to phosphorus deficiency. *Plant Physiol* 156: 1025–1032

Chiou T-J, Lin S-I (2011) Signaling network in sensing phosphate availability in plants. *Annu Rev Plant Biol* 62: 185–206

Constantin GD, Gronlund M, Johansen IE, Stougaard J, Lund OS (2008) Virus-induced gene silencing as a reverse genetic tool to study development of symbiotic root nodules. *Mol Plant Microbe Interact* 21: 720–727

Cordell D, Drangert J-O, White S (2009) The story of phosphorus: global food security and food for thought. *Glob Environ Change* 19: 292–305

Di Stilio VS, Kumar RA, Oddone AM, Tolkin TR, Salles P, McCarty K (2010) Virus-induced gene silencing as a tool for comparative functional studies in *Thalictrum*. *PLoS ONE* 5: e12064

Himber C, Dunoyer P, Moissiard G, Ritzenthaler C, Voinnet O (2003) Transitivity-dependent and -independent cell-to-cell movement of RNA silencing. *EMBO J* 22: 4523–4533

Holzberg S, Brosio P, Gross C, Pogue GP (2002) *Barley stripe mosaic virus*-induced gene silencing in a monocot plant. *Plant J* 30: 315–327

Hong JS, Rhee S-J, Kim E-J, Kim T-S, Ryu KH, Masuta C, Lee GP (2012) Application of a reassortant *Cucumber mosaic virus* vector for gene silencing in tomato and chili pepper plants. *Plant Pathol J* 28: 81–86

Hsieh M-H, Lu H-C, Pan Z-J, Yeh H-H, Wang S-S, Chen W-H, Chen H-H (2013) Optimizing virus-induced gene silencing efficiency with *Cymbidium* mosaic virus in *Phalaenopsis* flower. *Plant Sci* 201–202: 25–41

Huang C, Xie Y, Zhou X (2009) Efficient virus-induced gene silencing in plants using a modified geminivirus DNA1 component. *Plant Biotechnol J* 7: 254–265

Igarashi A, Yamagata K, Sugai T, Takahashi Y, Sugawara E, Tamura A, Yaegashi H, Yamagishi N, Takahashi T, Isogai M, et al. (2009) Apple latent spherical virus vectors for reliable and effective virus-induced gene silencing among a broad range of plants including tobacco, tomato, *Arabidopsis thaliana*, cucurbits, and legumes. *Virology* 386: 407–416

Kanazawa A, Inaba J-I, Shimura H, Otagaki S, Tsukahara S, Matsuzawa A, Kim BM, Goto K, Masuta C (2011) Virus-mediated efficient induction of epigenetic modifications of endogenous genes with phenotypic changes in plants. *Plant J* 65: 156–168

Karasawa A, Ito A, Okada I, Hase S, Ehara Y (1997) A possible role of RNA 2 of cucumber mosaic cucumovirus as a determinant of infection phenotype on cowpea. *Ann Phytopathological Soc Jpn* 63: 289–297

Kumagai MH, Donson J, Della-Cioppa G, Harvey D, Hanley K, Grill LK (1995) Cytoplasmic inhibition of carotenoid biosynthesis with virus-derived RNA. *Proc Natl Acad Sci USA* 92: 1679–1683

Liou MR, Huang YW, Hu CC, Lin NS, Hsu YH (2014) A dual gene-silencing vector system for monocot and dicot plants. *Plant Biotechnol J* 12: 330–343

Liu B, Watanabe S, Uchiyama T, Kong F, Kanazawa A, Xia Z, Nagamatsu A, Arai M, Yamada T, Kitamura K, et al. (2010) The soybean stem growth habit gene *Dt1* is an ortholog of Arabidopsis *TERMINAL FLOWER1*. *Plant Physiol* 153: 198–210

Liu E, Page JE (2008) Optimized cDNA libraries for virus-induced gene silencing (VIGS) using tobacco rattle virus. *Plant Methods* 4: 5

Livak KJ, Schmittgen TD (2001) Analysis of relative gene expression data using real-time quantitative PCR and the $2^{-\Delta\Delta C_T}$ method. *Methods* 25: 402–408

Matsuo K, Hong JS, Tabayashi N, Ito A, Masuta C, Matsumura T (2007) Development of *Cucumber mosaic virus* as a vector modifiable for different host species to produce therapeutic proteins. *Planta* 225: 277–286

Nagamatsu A, Masuta C, Senda M, Matsuura H, Kasai A, Hong JS, Kitamura K, Abe J, Kanazawa A (2007) Functional analysis of soybean genes involved in flavonoid biosynthesis by virus-induced gene silencing. *Plant Biotechnol J* 5: 778–790

Nagamatsu A, Masuta C, Matsuura H, Kitamura K, Abe J, Kanazawa A (2009) Down-regulation of flavonoid 3′-hydroxylase gene expression by virus-induced gene silencing in soybean reveals the presence of a threshold mRNA level

associated with pigmentation in pubescence. *J Plant Physiol* 166: 32–39

Netsu O, Hiratsuka K, Kuwata S, Hibi T, Ugaki M, Suzuki M (2008) Peanut stunt virus 2b cistron plays a role in viral local and systemic accumulation and virulence in *Nicotiana benthamiana*. *Arch Virol* 153: 1731–1735

Neumann G (2010) Mining for nutrients: regulatory aspects of cluster root function and development. *New Phytol* 187: 879–882

Obrepalska-Steplowska A, Budziszewska M, Pospieszny H (2008) Complete nucleotide sequence of a Polish strain of *Peanut stunt virus* (PSV-P) that is related to but not a typical member of subgroup I. *Acta Biochim Pol* 55: 731–739

O'Rourke JA, Yang SS, Miller SS, Bucciarelli B, Liu J, Rydeen A, Bozsoki Z, Uhde-Stone C, Tu ZJ, Allan D, et al. (2013) An RNA-Seq transcriptome analysis of orthophosphate-deficient white lupin reveals novel insights into phosphorus acclimation in plants. *Plant Physiol* 161: 705–724

Otagaki S, Arai M, Takahashi A, Goto K, Hong JS, Masuta C, Kanazawa A (2006) Rapid induction of transcriptional and post-transcriptional gene silencing using a novel *Cucumber mosaic virus* vector. *Plant Biotechnol* 23: 259–265

Peele C, Jordan CV, Muangsan N, Turnage M, Egelkrout E, Eagle P, Hanley-Bowdoin L, Robertson D (2001) Silencing of a meristematic gene using geminivirus-derived vectors. *Plant J* 27: 357–366

Pflieger S, Blanchet S, Camborde L, Drugeon G, Rousseau A, Noizet M, Planchais S, Jupin I (2008) Efficient virus-induced gene silencing in Arabidopsis using a 'one-step' TYMV-derived vector. *Plant J* 56: 678–690

Pflieger S, Richard MMS, Blanchet S, Meziadi C, Geffroy V (2013) VIGS technology: an attractive tool for functional genomics studies in legumes. *Funct Plant Biol* 40: 1234–1248

Reynolds A, Leake D, Boese Q, Scaringe S, Marshall WS, Khvorova A (2004) Rational siRNA design for RNA interference. *Nat Biotechnol* 22: 326–330

Robertson D (2004) VIGS vectors for gene silencing: many targets, many tools. *Annu Rev Plant Biol* 55: 495–519

Ryu CM, Anand A, Kang L, Mysore KS (2004) Agrodrench: a novel and effective agroinoculation method for virus-induced gene silencing in roots and diverse Solanaceous species. *Plant J* 40: 322–331

Sbabou L, Bucciarelli B, Miller S, Liu J, Berhada F, Filali-Maltouf A, Allan D, Vance C (2010) Molecular analysis of *SCARECROW* genes expressed in white lupin cluster roots. *J Exp Bot* 61: 1351–1363

Secco D, Shou H, Whelan J, Berkowitz O (2014) RNA-seq analysis identifies an intricate regulatory network controlling cluster root development in white lupin. *BMC Genomics* 15: 230

Senthil-Kumar M, Mysore KS (2011a) Virus-induced gene silencing can persist for more than 2 years and also be transmitted to progeny seedlings in *Nicotiana benthamiana* and tomato. *Plant Biotechnol J* 9: 797–806

Senthil-Kumar M, Mysore KS (2011b) New dimensions for VIGS in plant functional genomics. *Trends Plant Sci* 16: 656–665

Shen J, Yuan L, Zhang J, Li H, Bai Z, Chen X, Zhang W, Zhang F (2011) Phosphorus dynamics: from soil to plant. *Plant Physiol* 156: 997–1005

Suzuki M, Hibi T, Masuta C (2003a) RNA recombination between cucumoviruses: possible role of predicted stem-loop structures and an internal subgenomic promoter-like motif. *Virology* 306: 77–86

Suzuki M, Kuwata S, Kataoka J, Masuta C, Nitta N, Takanami Y (1991) Functional analysis of deletion mutants of cucumber mosaic virus RNA3 using an *in vitro* transcription system. *Virology* 183: 106–113

Suzuki M, Yoshida M, Yoshimura T, Hibi T (2003b) Interaction of replicase components between *Cucumber mosaic virus* and *Peanut stunt virus*. *J Gen Virol* 84: 1931–1939

Tian J, Pei H, Zhang S, Chen J, Chen W, Yang R, Meng Y, You J, Gao J, Ma N (2014) TRV–GFP: a modified *Tobacco rattle virus* vector for efficient and visualizable analysis of gene function. *J Exp Bot* 65: 311–322

Tian L, Peel GJ, Lei Z, Aziz N, Dai X, He J, Watson B, Zhao PX, Sumner LW, Dixon RA (2009) Transcript and proteomic analysis of developing white lupin (*Lupinus albus* L.) roots. *BMC Plant Biol* 9: 1

Tuttle JR, Idris AM, Brown JK, Haigler CH, Robertson D (2008) Geminivirus-mediated gene silencing from *Cotton leaf crumple virus* is enhanced by low temperature in cotton. *Plant Physiol* 148: 41–50

Uhde-Stone C, Zinn KE, Ramírez M, Li A, Vance CP, Allan DL (2003) Nylon filter arrays reveal differential gene expression in proteoid roots of white lupin in response to phosphorus deficiency. *Plant Physiol* 131: 1064–1079

Uhde-Stone C, Liu J, Zinn KE, Allan DL, Vance CP (2005) Transgenic proteoid roots of white lupin: a vehicle for characterizing and silencing root genes involved in adaptation to P stress. *Plant J* 44: 840–853

Ui-Tei K, Naito Y, Takahashi F, Haraguchi T, Ohki-Hamazaki H, Juni A, Ueda R, Saigo K (2004) Guidelines for the selection of highly effective siRNA sequences for mammalian and chick RNA interference. *Nucleic Acids Res* 32: 936–948

Valentine T, Shaw J, Block VC, Philipps MS, Oparka KJ, Lacomme C (2004) Efficient virus-induced gene silencing in roots using a modified tobacco rattle virus vector. *Plant Physiol* 136: 3999–4009

Vance CP (2010) Quantitative trait loci, epigenetics, sugars, and microRNAs: quaternaries in phosphate acquisition and use. *Plant Physiol* 154: 582–588

Vance CP, Uhde-Stone C, Allan DLP (2003) Phosphorus acquisition and use: critical adaptations by plants for securing a nonrenewable resource. *New Phytol* 157: 423–447

Varkonyi-Gasic E, Wu R, Wood M, Walton EF, Hellens RP (2007) Protocol: a highly sensitive RT-PCR method for detection and quantification of microRNAs. *Plant Methods* 3: 12

Yamagishi M, Kishimoto S, Nakayama M (2010) Carotenoid composition and changes in expression of carotenoid biosynthetic genes in tepals of Asiatic hybrid lily. *Plant Breed* 129: 100–107

Yamagishi M, Zhou K, Osaki M, Miller SS, Vance CP (2011) Real-time RT-PCR profiling of transcription factors including 34 MYBs and signaling components in white lupin reveals their P status dependent and organ-specific expression. *Plant Soil* 342: 481–493

Yan H-X, Fu D-Q, Zhu B-Z, Liu H-P, Shen X-Y, Luo Y-B (2012) Sprout vacuum-infiltration: a simple and efficient agroinoculation method for virus-induced gene silencing in diverse solanaceous species. *Plant Cell Rep* 31: 1713–1722

Yan LY, Xu ZY, Goldbach R, Kunrong C, Prins M (2005) Nucleotide sequence analyses of genomic RNAs of *Peanut stunt virus* Mi, the type strain representative of a novel PSV subgroup from China. *Arch Virol* 150: 1203–1211

Yuan C, Li C, Yan L, Jackson AO, Liu Z, Han C, Yu J, Li D (2011) A high throughput barley stripe mosaic virus vector for virus

induced gene silencing in monocots and dicots. *PLoS ONE* 6: e26468

Zhang C, Bradshaw JD, Whitham SA, Hill JH (2010) The development of an efficient multipurpose Bean pod mottle virus viral vector set for foreign gene expression and RNA silencing. *Plant Physiol* 153: 52–65

Zhong X, Yuan X, Wu Z, Khan MA, Chen J, Li X, Gong B, Zhao Y, Wu J, Wu C, et al. (2014) Virus-induced gene silencing for comparative functional studies in *Gladiolus hybridus*. *Plant Cell Rep* 33: 301–312

Zhou K, Yamagishi M, Osaki M, Masuda K (2008) Sugar signalling mediates cluster root formation and phosphorus starvation-induced gene expression in white lupin. *J Exp Bot* 59: 2749–2756

Zhu Y, Yan F, Zörb C, Schubert S (2005) A link between citrate and proton release by proteoid roots of white lupin (*Lupinus albus* L.) grown under phosphorus-deficient conditions? *Plant Cell Physiol* 46: 892–901

Zhu Y, Zeng H, Dong C, Yin X, Shen Q, Yang Z (2010) microRNA expression profiles associated with phosphorus deficiency in white lupin (*Lupinus albus* L.). *Plant Sci* 178: 23–29

Supplementary Table 1 Primers for *PDS* fragment amplification

Primer name	Orientation	Sequence (5′ to 3′)
NbPDShMf	forward	GCGACGCGTTTGGTACGAGACTGGGTTGC
NbPDSiXr	reverse	GCGTCTAGATGCATATTTGGGTAAGCCCC
NbPDSaMf	forward	GCGACGCGTGCGATGCCTAACAAGCCAGG
NbPDSbXr	reverse	GCGTCTAGAGCTTCAGGAAAATCAAAGCGG
NbPDScMf	forward	GCGACGCGTGCTATTGGACTCTTGCCAGC
NbPDSdXr	reverse	GCGTCTAGAGCTTCAACATAAGATTGCCC
NbPDSeMf	forward	GCGACGCGTGCCTGATAGGGTGACAGAT
NbPDSfXr	reverse	GCGTCTAGATAAGTGCCTTTGACATGGC
NbPDSgXr	reverse	GCGTCTAGACAATCAAAATGCACTGCATCG
LaPDSeXf	forward	GCGTCTAGAGTTGAGGCTCAAGATGGCC
LaPDSgMr	reverse	GCGACGCGTGAGTGCCTTTGACATTGC
LaPDShMf	forward	GCGACGCGTGCAATTGGACTTCTGCCAGC
LaPDSiXr	reverse	GCGTCTAGACTCGTTCAGGAATGCCCTGC
LaPDSjMf	forward	GCGACGCGTCTGAACGAGTAACTGATGAGG
LaPDSkXr	reverse	GCGTCTAGAGCAATCAATACACATTGCATTG

*Xba*I (TCTAGA) and *Mlu*I (ACGCGT) restriction sites are underlined.

Note:
Primers NbPDShMf and NbPDSiXr amplified NbPDS-A (51 bp).
Primers NbPDSaMf and NbPDSbXr amplified NbPDS-B (50 bp).
Primers NbPDScMf and NbPDSdXr amplified NbPDS-C (50 bp).
Primers NbPDSeMf and NbPDSfXr amplified NbPDS-D (50 bp).
Primers NbPDSeMf and NbPDSgXr amplified NbPDS-2 (95 bp).
Primers NbPDScMf and NbPDSfXr amplified NbPDS-3 (145 bp).
Primers NbPDScMf and NbPDSgXr amplified NbPDS-4 (190 bp).
Primers NbPDSaMf and NbPDSgXr amplified NbPDS-5 (319 bp).
Primers NbPDShMf and NbPDSgXr amplified NbPDS-6 (434 bp).

Primers LaPDSeXf and LaPDSgMr amplified LaPDS-1 (102 bp).
Primers LaPDShMf and LaPDSiXr amplified LaPDS-2 (106 bp).
Primers LaPDSjMf and LaPDSkXr amplified LaPDS-3 (94 bp).

```
         1                                                          60
LaPDS1   AAAGGTTGCTGCATGGCAAGATGAAGATGGAGACTGGTATGAGACAGGCCTACACATATT
LaPDS2   AAAGATTGCTGCATGGCAAGATCAAGATGGGGACTGGTATGAGACAGGTCTACATATATT
         **** ********************* ******* ********************* ***** *****

        61                                                         120
LaPDS1   CTTTGGGGCTTACCCTAACGTACAGAACCTGTTTGGAGAACTTGGTATTAGTGATCGATT
LaPDS2   CTTTGGGGCTTACCCTAATATACAGAACCTGTTTGGAGAACTTGGTATTAATGATCGGTT
         ******************  ****************************** ****** **

       121                                                         180
LaPDS1   ACAATGGAAGGAGCATTCTATGATTTTTGCAATGCCAAATAAGCCTGGAGAATTTAGTCG
LaPDS2   ACAATGGAAGGAACATTCTATGATTTTTGCAATGCCAAACAAGCCTGGCGAATTTAGTCG
         *********** ************************ ******** ***********

       181                                                         240
LaPDS1   ATTTGATTTTCCCGACATCCTTCCATCTCCTTTAAACGGAATATGGGCAATATTGAGGAA
LaPDS2   GTTTGATTTTCCGGACGTCCTTCCTGCTCCATTAAATGGAATATGGGCAATATTGAAGAA
          ********** *** *******  **** ***** ****************** ***

       241                                                         300
LaPDS1   CAATGAAATGCTCACTTGGCCAGAGAAAGTCAAATTTGCAATTGGACTTCTGCCAGCTAT
LaPDS2   CAATGAGATGCTGACTTGGCCAGAGAAAGTCAAATTTGCAATTGGACTTCTGCCAGCCAT
         ****** ***** ****************************************** **

       301                                                         360
LaPDS1   GCTCGGTGGACAGCCTTATGTTGAGGCTCAAGATGGCCTTTCTGTTGAAGAATGGATGAA
LaPDS2   GCTTGGTGGGCAGCCTTATGTTGAGGCTCAAGATGGCCTTTCTGTTGAAGAATGGATGAA
         *** ***** **************************************************

       361                                                         420
LaPDS1   AAAGCAGGGCATTCCTGAACGAGTAACTGATGAGGTGTTCATAGCAATGTCAAAGGCACT
LaPDS2   AAAGCAGGGCATTCCTGAACGAGTAACTGATGAAGTTTTCATAGCAATGTCAAAGGCACT
         ********************************** ** **********************

       421                                                         480
LaPDS1   CAACTTCATCAACCCTGATGAACTTTCAATGCAATGTGTATTGATTGCTTTAAACAGATT
LaPDS2   CAACTTCATCAACCCTGATGAACTTTCAATGCAATGTATATTGATTGCTTTAAACCGATT
         ************************************ ***************** ****

       481                         505
LaPDS1   TCTTCAGGAGAAACATGGTTCTAAG
LaPDS2   TCTTCAGGAGAAGCATGGTTCTAAG
         ************ ************
```

Supplementary Figure 1 Nucleotide sequence alignment of *LaPDS1* and *LaPDS2* (partial).